# A lipoprotein-containing particle is transferred from the serum across the mammary epithelium into the milk of lactating mice

**Jenifer Monks,* Patricia Uelmen Huey,† Linda Hanson,* Robert H. Eckel,† Margaret C. Neville,[1,*] and Sean Gavigan***

Department of Physiology and Biophysics,* University of Colorado Health Sciences Center, Denver, CO 80262 and Department of Medicine,† Division of Endocrinology, Metabolism and Diabetes, University of Colorado Health Sciences Center, Denver, CO 80262

**Abstract** **To investigate the role of low-density lipoprotein (LDL) in the delivery of cholesterol to the mammary gland during pregnancy and lactation, we examined the distribution of radioactivity from $^{125}$I-tyramine cellobiose-LDL injected into the tail vein of female mice at various stages of the reproductive cycle. Changes in the proportion of isotope taken up by the mammary gland largely reflected the increased weight of the gland in pregnancy and lactation. In addition, during lactation, radioactivity was found in the milk and was associated with a protein of the molecular weight of apoB-100. Quantitatively similar results were obtained with mice homozygous for disruption of the LDL receptor gene (LDLR null). Analysis of endogenous lipoproteins showed that the milk lipoprotein particles were denser than the corresponding serum lipoproteins and largely depleted of triglyceride and cholesterol. Using fluorescence microscopy we visualize the sorting of apoB protein from the LDL lipid phase at the basal surface of the mammary epithelial cell of both wild-type and LDLR-null mice. Our findings provide evidence that the mammary epithelium of the lactating mouse is able to take up LDL from the plasma by a non-LDLR-mediated process. An apoB-containing particle from which the cholesterol has been removed is transferred into milk.**—Monks, J., P. U. Huey, L. Hanson, R. H. Eckel, M. C. Neville, and S. Gavigan. **A lipoprotein-containing particle is transferred from the serum across the mammary epithelium into the milk of lactating mice.** ***J. Lipid Res.*** **2001.** 42: **686–696.**

**Supplementary key words** mammary gland • cholesterol • epithelium • LDL • LDLR-null mice • transcytosis • lipoprotein metabolism • milk secretion

Although there has been considerable concern about the lipid content of dairy products, research has focused on the mechanisms of triglyceride secretion into milk (1–3); relatively little attention has been paid to the mechanisms responsible for cholesterol transfer. The mammary alveolar cell must supply cholesterol to the secreted milk fat globule and to replace apical membrane, suggesting that the mammary gland should have an increased cholesterol requirement during lactation. Popjak et al. (4) demonstrated that mammary epithelial cells are capable of synthesizing cholesterol de novo, and a role has been shown for lipoproteins in delivering cholesterol to the mammary gland (5, 6). However, because these reports predate any understanding of the mechanisms of cellular cholesterol trafficking, we initiated a study of low-density lipoprotein (LDL) metabolism in the mouse mammary gland.

The best understood pathway for cholesterol uptake by cells utilizes the LDL receptor (LDLR), shown by Goldstein et al. (7) to recognize the apolipoprotein (apo)B protein moiety of LDL (8). After binding, the LDL is internalized into the endocytic compartment where a decrease in pH leads to the dissociation of LDL from the receptor, allowing recycling of the receptor to the cell surface. The lipoprotein is targeted to the lysosomes for degradation of both the protein and lipid components. Cholesterol released by this process is available for membrane synthesis or storage as cholesterol ester. Accumulation of excess cholesterol is prevented by the down-regulation of LDLR expression. More recently it has been shown that some cells, including hepatocytes and steroidogenic cells, also accumulate cholesterol from high-density lipoprotein (HDL) and LDL via a selective uptake pathway utilizing scavenger receptors (9–13). In

Abbreviations: ACAT, acyl coenzyme A: cholesterol acyl-transferase; CD36, cluster determinant 36; DAPI, 4α, 6-diamidino-2-phenylindole; DiI, 1,1′-dioctadecyl-3,3,3′,3′-tetramethylindocarbocyanine perchlorate; EDTA, ethylenediaminetetraacetic acid; FITC, fluorescein; HDL, high density lipoprotein; HSPG, heparan sulfate proteoglycan; LDL, low-density lipoprotein; LDLR, low-density lipoprotein receptor; MLP, milk lipoprotein particle; $NaN_3$, sodium azide; NPNL, nonpregnant and nonlactating; PMSF, phenylmethylsulfonyl fluoride; SR-B1, scavenger receptor, class B, type I; TCA, trichloroacetic acid; TC-LDL, tyramine cellobiose labeled LDL; VLDL, very low-density lipoprotein.

[1] To whom correspondence should be addressed at Department of Physiology and Biophysics, 4200 East Ninth Avenue, C-240, University of Colorado Health Sciences Center, Denver, CO 80262.
e-mail: Peggy.Neville@UCHSC.edu

this pathway, cholesterol ester is taken up from a cell-surface bound lipoprotein without internalization of the particle and subsequent breakdown of the protein moiety.

To test the hypothesis that the mammary epithelial cell acquires cholesterol from LDL by the LDLR pathway, we studied the uptake of $^{125}$I-tyramine cellobiose LDL ($^{125}$I-TC-LDL) in virgin, pregnant, and lactating mice. The sugar moiety of this molecule does not interfere with LDL transport; however, it is not degraded in the lysosomes, and accumulation of radioactivity within tissues is generally proportional to the total LDL uptake over the the study period (14, 15). The unexpected finding that the radioactivity was transferred extensively into the milk prompted us to determine that apoB-containing particles in the LDL size range are present in mouse milk, with the cholesterol having been scavenged prior to or during transport across the mammary epithelium. To determine whether the LDLR is involved in this uptake, we examined the interaction of labeled LDL with the mammary gland of normal and LDLR-null mice.

## MATERIALS AND METHODS

### Mice

CD-1 mice (Charles River Labs, Wilmington, MA) were used for most experiments. To examine the role of the LDLR, mice homozygous for a targeted disruption of the LDLR gene (16, 17) were used (Jackson Labs, Bar Harbor, ME). For these experiments, the control mice were B6-129 mice (JacksonLabs), the same strain as the LDLR-null mice. All mice were housed in the University of Colorado Health Sciences Center USDA-approved Center for Laboratory Animal Care. Breeding was timed by the observation of a vaginal plug; day 1 of pregnancy was the day the plug was observed. Day 1 of lactation was the day the pups were born. At birth, litters were standardized to 10 pups. All experiments were performed in mid-lactation (between days 7 and 14) with most performed on day 10. In some experiments, virgin or pregnant animals were used. The Institutional Animal Care and Use Committee of the University of Colorado Health Sciences Center approved all procedures.

### Preparation of lipoproteins

Human LDL were prepared using preparative density ultracentrifugation (18). In earlier experiments, plasma was collected from normal volunteers or from a patient undergoing plasmapheresis in treatment for Type II b hyperlipidemia. After centrifugation at 50,000 rpm in a 60Ti rotor (Beckman Instruments, Inc., Palo Alto, CA) for 16 h, very low-density lipoprotein (VLDL) was removed from the top of the tube with a syringe and hypodermic needle. VLDL-depleted plasma was adjusted to a density of 1.30 g/ml with KBr, and tubes were prepared in which 15 ml of plasma was layered under 25 ml of saline (density 1.006 g/ml). These tubes were centrifuged at 50,000 rpm for 2.5 h in a VAC 50 rotor (Beckman), during which time a density gradient formed in the tubes. LDL formed a tight band close to the top of the tube and was removed with a syringe. LDL was recentrifuged at density 1.065, dialyzed, sterilized by filtration through a 0.22-micrometer filter, and stored at 4°C. The protein concentration was assayed using the BCA reagent kit (Pierce, Rockford, IL). In later experiments, human LDL was purchased from Biomedical Technologies (Stoughton, MA).

TC was synthesized and purified as described by Pittman et al. (14, 15) and then labeled with $^{125}$I (ICN, Costa Mesa, CA) using iodobeads (Pierce Biochemical Co., Rockford, IL). One iodobead was preincubated for 5 min with 1-mCi Na$^{125}$I in 100 μl of 20 mM sodium phosphate buffer (pH 7.2). TC (100 nmol) in 100 μl of the same buffer was added for a further 10 min. Transferring the solution to a fresh tube and adding 5-μl 100 mM KI and 100 mM sodium bisulfite stopped the reaction. The $^{125}$I-TC was covalently coupled to the apoB moiety of human LDL essentially by the method of Pittman et al. (14, 15). Directly radioiodinated LDL was also prepared, following the standard Pierce iodobead protocol. Unincorporated $^{125}$I or $^{125}$I-TC was removed by gel filtration with a Sepharose G-50 column (Amersham Pharmacia Biotech, Inc., Piscataway, NJ) and dialysis, first against 0.1 M ammonium bicarbonate, and then extensively against Dulbecco's phosphate buffered saline (PBS). Labeled LDL was used within 24 h of labeling. More than 98% of the radioactivity in the injectate and the blood following the experiment was precipitable with trichloroacetic acid.

### $^{125}$I-TC-LDL transfer to mammary gland, milk, and liver in CD-1 mice

Virgin, pregnant (day 14), and lactating (day 10) female CD-1 mice were warmed under a heat lamp for 5 min to dilate the tail veins, placed in a restraining apparatus, and injected with 100–200 μl of $^{125}$I-TC-LDL (50–100 μg protein, 6 million cpm) or $^{125}$I-LDL (50–100 μg protein, 1–2 × $10^8$ million cpm) into a lateral tail vein. Blood samples (10–20 μl) were taken from the tail vein hourly for 7 to 9 h and assayed for radioactivity (data not shown). $^{125}$I-TC-LDL and $^{125}$I-LDL were cleared exponentially from the plasma of lactating mice with mean rate constants of $-0.102 \pm 0.016$ and $-0.111 \pm 0.008$ $h^{-1}$, respectively (equivalent to a half-time of 5 h), giving us confidence that the coupling with $^{125}$I-TC did not significantly alter the whole-body metabolism of the LDL. The rate constant of loss of LDL from the plasma was similar in virgin, pregnant, and lactating mice. The pups were removed from the lactating mice 6 or 7 h after isotope injection. Milk was manually collected 1 h later from anaesthetized dams after oxytocin injection (0.01 USP units/g body weight). A belled Pasteur pipette attached to a house vacuum line was used to provide suction. After milk removal, the mice were deeply anesthetized with pentobarbital and perfused with 30-ml ice-cold Ringer solution through the left ventricle of the heart. The liver and 4th and 5th mammary glands were then removed, weighed, homogenized in 0.2 M tris (hydroxymethyl) aminomethane buffer (pH 8.2) with 0.02 M sucrose, 1% bovine serum albumin (BSA), 0.0125% heparin, 0.5% deoxycholate, and 0.02% NP-40, and the homogenate was assayed for content of radioactivity. Mammary glands 1 through 3 were also removed for weighing to provide a basis for calculating the utilization of labeled LDL by the entire set of mammary glands.

### Determination of interstitial radioactivity

To determine the fraction of radioactivity in the interstitial space of the mammary gland and liver, strips ~1 mm in diameter and 1 to 2 cm in length were cut from the tissues of mice that had been injected 8 h previously with $^{125}$I-TC-LDL and perfused with Ringer's solution as described above. These tissue pieces were washed through a series of tubes containing ice-cold PBS at timed intervals as described previously (19). After 1 h the tissue piece was placed in water containing 0.1% triton and incubated at 37°C overnight to remove residual radioactivity. The radioactivity in each tube was counted and added successively to the residual to produce efflux curves like those shown in **Fig. 1A**. We have shown previously in muscle (20) and mammary gland (19) that such curves can be fit with a double exponential curve with a fast fraction representing interstitial solute and a slow fraction representing cellular solute. Curves like those shown in Fig. 1A were obtained for the livers and mammary glands from two virgin, two

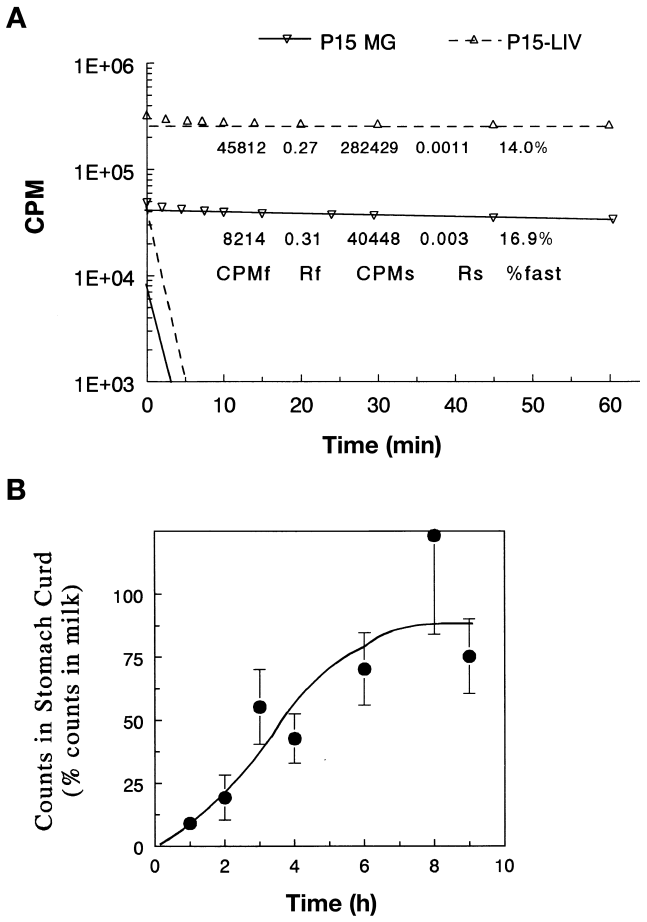


**Fig. 1.** A: Counts remaining in mammary gland (MG) and liver strips from mice injected with $^{125}$I-tyramine cellobiose low-density lipoprotein ($^{125}$I-TC–LDL) 8 h previously and washed through a series of tubes containing ice-cold phosphate-buffered saline. Representative curves are shown for liver (dotted lines) and mammary gland (solid lines) from pregnant mice. The curves were fit to a double exponential and the two components of the exponential plotted. The coefficients for the counts in the fast and slow fractions (CPMf and CPMs, respectively) and the rate constants in $h^{-1}$ (Rf and Rs, respectively) are shown with the percentage of the total counts in the fast fraction for each of these representative curves. Tissues from six mice at various reproductive stages were subjected to this treatment, and similar curves were obtained from all. B: Appearance of radioactivity in the stomach contents of pups after injection of $^{125}$I-LDL or $^{125}$I-TC LDL in the dam. Dams were injected intravenously with $19 \times 10^6$ ($^{125}$I-TC LDL) or $16 \times 10^6$ ($^{125}$I-LDL) cpm (2 dams each probe). Pups were removed from the dam at intervals for 30 min and replaced with the dams for 60 min so that the stomachs would contain mostly recently secreted milk. There was no essential difference between the results obtained from the two probes, so average values ± SEM are presented as a percentage of the counts in the milk from the same dam.

pregnant, and two lactating mice. Neither the fraction of radioactivity in the fast fraction nor the mean residual interstitial space differed with reproductive stage, so the results were pooled to give a mean fast fraction of 18.5 ± 1.5% and 11.1 ± 2.0% of total radioactivity in the liver and mammary gland, respectively. The amount of radioactivity in the fast fraction was equivalent to a residual interstitial space after perfusion of 2.5 ± 0.4 μl/g in the mammary gland and 7.9 ± 1.5 μl/g in the liver. These values were used with blood counts at the termination of the experiment to correct data from other experiments.

### Time course of $^{125}$I-TC-LDL accumulation in milk

To examine the rate of appearance of radioactivity in the milk, we took advantage of the superior ability of mouse pups to remove milk from the gland at intervals following injection of $^{125}$I-TC-LDL into the lactating dams. Prior to each time point one pup was removed for 30 min to allow some emptying of the milk within the stomach. The pup was marked, returned to its mother to suckle for 60 min, euthanized, and the stomach was removed to assay the coagulated milk for radioactivity. Radioactivity could be detected in the stomachs within 1 h of injection and increased steadily for the next 3–4 h before reaching a steady state between 75 and 100% of the concentration of counts in milk (Fig. 1B). The results of this experiment were used to determine that a pseudo-steady state of labeled LDL in the milk was achieved within the 8-h experiment.

### Milk fractionation

Milk was collected and centrifuged at 3,000 rpm at 4°C for 15 min using a Hermle 220.59V rotor and centrifuge (National Labnet Co., Woodbridge, NJ). Skimmed milk was removed from beneath the solidified fat cake with a Pasteur pipette and further centrifuged at 14,000 rpm for 1 h at 4°C using the same Hermle rotor and centrifuge. This procedure resulted in the formation of a tight casein pellet, a loose membrane pellet, and the soluble whey fraction. Whey was removed with a syringe; 500-μl aliquots of whole milk, skimmed milk, and whey were incubated with 250-μl trichloroacetic acid (TCA) (25%) and centrifuged at 1,000 rpm for 20 min. Radioactivity was assayed in the unprecipitated samples and in the TCA-soluble and -precipitated fractions by gamma counting.

### Sequential density centrifugation to prepare LDL

All lipoprotein analyses were performed on mice fed ad libitum, with milk and serum samples collected mid-day. Lactating mice that are fasted either shut down milk production immediately or are overly stressed, so milk samples could not be reliably obtained from these mice.

To determine the density of the apoB-containing particles using sequential ultracentrifugation, 1-ml aliquots of pooled whey and serum [1 mM ethylenediaminetetraacetic acid (EDTA), 1 mM phenylmethylsulfonyl fluoride (PMSF), 0.02% $NaN_3$] were adjusted to a density of 1.020 g/ml with NaBr and ultracentrifuged at 50,000 rpm for 16 h at 15°C in a Beckman TL 100.3 rotor to float VLDL, IDL, and chylomicrons. A common fraction was removed from the top of each tube. Bottom fractions were adjusted to a density of 1.065 g/ml with NaBr and recentrifuged under the same conditions. Top and bottom fractions were again collected, dialyzed overnight against PBS (1 mM EDTA, 1 mM PMSF, 0.02% $NaN_3$), and analyzed for apoB by immunoblot analysis.

### Liquid chromatographic separation of lipoproteins

Separation of plasma lipoproteins was accomplished using a Beckman System Gold liquid chromatography apparatus, consisting of a 126-nm solvent module, a 166-nm UV detector, an automated fraction collector, and two Superose-6 gel permeation columns (Amersham Pharmacia Biotech, Inc., Piscataway, NJ) linked in series (21). A volume of 0.20 ml of either serum or whey was applied onto the columns and eluted in aqueous buffer (154 mM NaCl, 0.02% $NaN_3$, 1 mM EDTA) at a constant flow rate of 0.4 ml/min. The individual lipoprotein peaks were detected by UV absorbance (280 nm), collected in 0.4-ml aliquots, and analyzed for total cholesterol and triglycerides using commercially available kits (Cholesterol CII and Triglyceride E kits, respectively; Wako BioProducts, Richmond, VA). The same kit was used for assay of total cholesterol in milk, whey, and serum.

### Immunoblotting for mouse apoB

Serum, whey, and density gradient or fast protein liquid chromatography (FPLC)-fractionated samples were resolved on 8% or 12% Prosieve (FMC Bioproducts, Rockland, ME) gels by the method of Ishibashi et al. (17), except that lipoproteins were not delipidated, and transferred to Hybond-C extra, nitrocellulose (Amersham). Membranes were blocked with 0.8% gelatin in PBS + 0.1% Tween 20. Primary antibody was a goat-anti-rat LDL serum (a generous gift of Dr. Paul Roheim, Louisiana State University), diluted 1:500, which recognizes both mouse apoB-48 and apoB-100, detected using a rabbit-anti-goat IgG, peroxidase conjugate (Sigma, St. Louis, MO), and ECL Supersignal reagent (Pierce Biochemical Co., Rockford, IL). For quantitation of the ratio of whey to serum apoB, 1, 2, and 5 μl of whey were mixed with sample buffer, run on gels, transferred to nitrocellulose, and blotted with the same antibody. After detection with the ECL reagent at times that did not saturate the signal on the X-ray film, the radiographs were scanned, and the density of the apoB-48 and apoB-100 bands was quantitated using SlideBook software (Intelligent Imaging Innovations, Inc., Denver, CO).

### Density-gradient fractionation of lipoproteins

Pooled whey and serum from lactating CD-1 mice were dialyzed overnight against PBS (1 mM EDTA, 1 mM PMSF, 0.02% $NaN_3$) adjusted to a density of 1.042 g/ml with NaBr(18). This solution was layered between equal volumes of PBS adjusted to densities of 1.024 and 1.054 g/ml with NaBr and centrifuged at 40,000 rpm for 30 h at 15°C using a Beckman SW41Ti rotor. Fractions (0.5 ml) were collected from the top. The density of each fraction was determined using refractometry on salt and buffer-only gradient fractions. Fractions were analyzed for phospholipids using the Wako Phospholipids B kit (Wako BioProducts, Richmond, VA).

### Fluorescent LDL uptake

1,1′-Dioctadecyl-3,3,3′,3′-tetramethylindocarbocyanine perchlorate (DiI)-LDL (Molecular Probes, Eugene, OR) was labeled on the apoB protein using NHS-fluorescein kit (Pierce Biochemical Co., Rockford, IL) according to the manufacturer's instructions. The fluorescein (FITC)-DiI-LDL was dialyzed against Kreb's Ringer phosphate buffer (Ringer's) overnight. Just prior to the experiment, the FITC-DiI-LDL was sterile filtered (0.22 micrometers) to remove large aggregates. A lactating mouse was anaesthetized with sodium pentobarbital (0.1 mg/g body weight, with 1-mg boosts as necessary). The skin covering the fourth and fifth mammary glands on one side was pulled back and pinned to expose the glands, which were overlaid with the FITC-DiI-LDL probe in Ringer's (+0.5% fetal calf serum). Incubation continued for 2 h, during which the mouse was kept warm and moist. At the end of the incubation, the bath solution was removed, the gland was rinsed briefly, and the mouse was perfused by intracardiac infusion with ice-cold Ringer's followed by 2% then 4% paraformaldehyde in Ringer's. The dissected mammary gland was further fixed in 4% paraformaldehyde at 4°C overnight. Tissue was then pressed in aluminum foil, frozen in isopentane, cooled with liquid nitrogen, and stored at −70°C.

Sections of 6–16 mm were prepared from frozen tissue using a Damon/IEC division minotome and placed on Cell-Tak (Collaborative Biomedical Products, Bedford, MA) coated coverslips. Upon rewarming, sections were further fixed in 3% paraformaldehyde, 3% sucrose for 15 min, rinsed with PBS, and mounted in glycerol-based mounting medium containing 2-mg/ml o-phenylenediamine (antifade) and 0.6-μg/ml 4α, 6-diamidino-2-phenylindole (DAPI).

Images were collected using SlideBook software (Intelligent Imaging Innovations, Inc., Denver, CO) on a Nikon Diaphot TMD microscope equipped for fluorescence with a Xenon lamp and filter wheels (Sutter Instruments, Novato, CA), fluorescent filters (Chroma, Brattleboro, VT), cooled CCD camera (Cooke, Tonawanda, NY), and stepper motor (Intelligent Imaging Innovations, Inc., Denver, CO). Multi-fluor images were merged, deconvolved, and renormalized using SlideBook software.

Quantitation of fluorescent localization was performed using SlideBook. Briefly, segmenting the image generated a mask representing the total fluorescence in a channel, selecting all regions where the signal was significantly over background. The total area of this fluorescence, as well as the integrated fluorescence intensity in the mask, was then calculated. Background subtraction was performed using the average intensity/pixel in "empty" or nonstained areas of the cell. Areas of membrane or intracellular staining were hand-delineated, and the integrated fluorescence intensity for each fluor in the resulting subcellular locales was used to generate the ratios cited in the text. These ratios were then compared between many images to obtain the mean and standard deviation. This method of generating quantitative data from fluorescent images has been described by Ghosh et al. (22, 23).

## RESULTS

### Effect of reproductive state on $^{125}$I-TC-LDL uptake in the mammary gland

Uptake of LDL by the mammary gland and liver was studied at various reproductive stages by measuring the accumulated radioactivity 8 h after intravenous injection of human LDL labeled with $^{125}$I-TC. We anticipated that internalized LDL would be degraded in lysosomes providing cholesterol for mammary growth during pregnancy and secretion into milk during lactation. The labeled sugar moiety would remain behind, providing a measure of cumulative LDL uptake. Unexpectedly, although the ratio of intracellular counts to serum counts decreased in the liver, the radioactivity in the mammary gland, expressed as a similar ratio to the serum, remained relatively constant in the three reproductive stages (**Fig. 2A**). More unexpectedly, a substantial amount of radioactivity was also detected in the milk. The radioactivity in the blood was greater than 98% TCA precipitable (Fig. 2B). In the liver and milk, 85 to 90% was TCA precipitable. In the mammary gland, the TCA-precipitable radioactivity increased from 67% in the virgin gland to 85% in the lactating gland. Of the TCA-soluble radioactivity, 25–45% represented free iodide; the rest was assumed to represent tyramine cellobiose hydrolyzed from the apoB. Thus, in lactation, only about 8% of the radioactivity in the mammary gland represented free, labeled tyramine cellobiose. When the LDL was directly labeled with $^{125}$I, a much greater proportion of the radioactivity in the mammary gland was free iodine, probably because the iodinase in the mammary gland is quite efficient at removing iodide groups from tyrosine (24). Nevertheless, TCA-precipitable radioactivity was found in the milk (data not shown).

Expressing the data as the ratio of the tissue to the blood concentration does not give a real representation of changes in LDL metabolism with reproductive state because there are large increases in organ weight associated with pregnancy and lactation, as shown in **Fig. 3A**. Thus, liver weight nearly doubled during this period, and the weight of the mammary gland increased fivefold from the virgin state to lactation. When the total amount of label

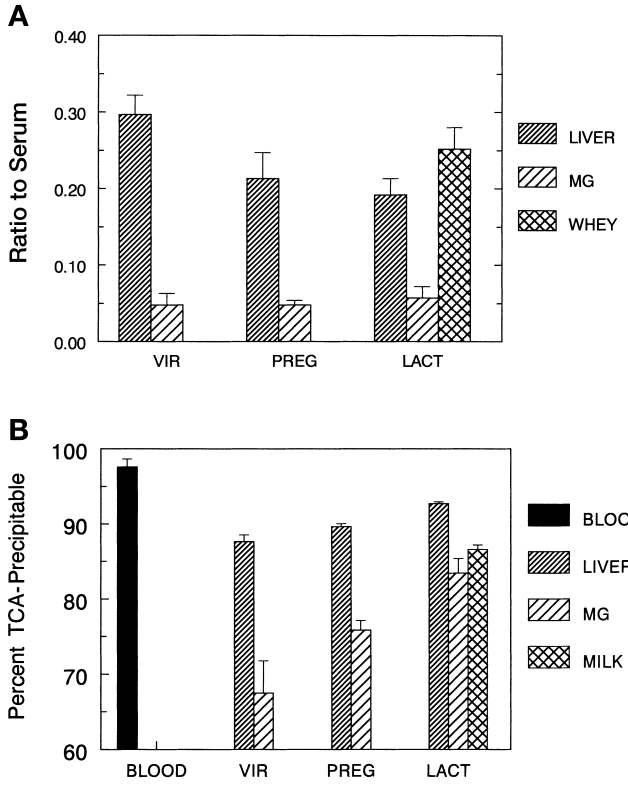


**Fig. 2.** A: Accumulation of $^{125}$I in liver and mammary gland (MG) of virgin (VIR; n = 5), 14-day pregnant (PREG; n = 4), and 10-day lactating (LACT; n = 5) mice 8 h after intravenous injection of $^{125}$I-TC-LDL. The ratio of whey to serum is also shown for lactating mice (n = 3). Data are shown as mean and SEM of the ratio of counts per gram of mammary gland to counts per gram of serum. Counts are corrected for interstitial radioactivity as described in Materials and Methods. B: TCA-precipitable radioactivity as a percentage of the total radioactivity in the tissues of the animals from A.

taken up by all the mammary glands and the liver was calculated from the organ weights and expressed as percentage of injected dose, uptake into the mammary gland increased more than sixfold over the virgin when secretion into milk and mammary content are included (Fig. 3B), and uptake into the liver decreased by one third.

### $^{125}$I-TC-LDL uptake in LDLR-null mice

To determine whether the LDLR was involved in the extensive uptake of $^{125}$I-TC-LDL into the mammary gland and transfer into milk, the levels of radioactivity in the liver, mammary gland, and milk were examined 8 h after injection into LDLR-null mice and controls of the same strain. The results, again plotted as the percentage of injected dose taken up into each organ or into milk (**Fig. 4**), show that the proportion of labeled LDL in the mammary gland and secreted into milk was not significantly different in controls and knockout strains. About three times as much radioactivity was taken into the liver as into the mammary gland of the control mice. Uptake was decreased in the null strain, but the variability between mice was such that the difference did not reach significance. This experiment provides evidence that the transfer of the apoB moiety of LDL into the lactating mammary gland and milk is not dependent on the presence of the LDLR.

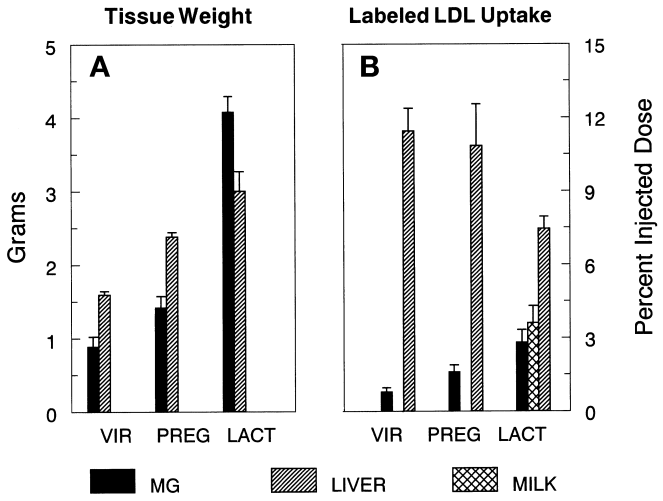


**Fig. 3.** Changes in organ weight and total $^{125}$I-TC-LDL uptake by mammary gland (MG) and liver during the reproductive cycle. A: The total weight of the mammary gland and liver in virgin, 14-day pregnant, and lactating mice. B: Labeled LDL uptake in the mammary gland and liver of the mice described in Fig. 2. Uptake was calculated from the ratio of the total counts in the tissue to the total counts injected. The total transfer into milk was calculated as the product of the concentration of activity in the milk and the volume of milk calculated to be secreted in 7 h. We used a figure of 1.5 g of milk secreted per gram of tissue (25) in making this calculation.

### Distribution and state of $^{125}$I in milk

To determine the distribution of radioactivity from the $^{125}$I-TC-LDL in the milk, we assayed the radioactivity in whole and skim milk, post-centrifugation whey, and the casein pellet, separated as described in Materials and Methods. Approximately 75% of the radioactivity in each fraction was precipitable by TCA, indicating that the bulk of the radioactivity was still associated with protein. The skim fraction contained approximately 80% of the counts observed in whole milk, indicating that unlike cholesterol, of which 80% is associated with the milk fat globule (26), relatively little radioactive apoB protein was associated with the milk fat. Indeed, the milk fat and casein pellet each

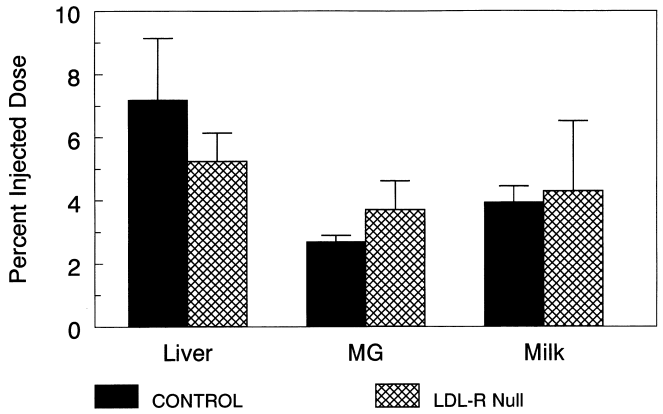


**Fig. 4.** $^{125}$I-TC-LDL uptake in LDLR-null mice. The results show means and SEM from five each null and wild-type mice of the same strain calculated as the percent-injected dose as in Fig. 3.

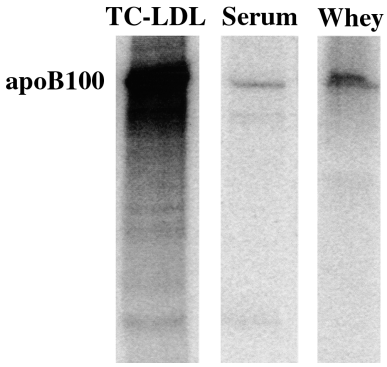


**Fig. 5.** Intact $^{125}$I-TC-labeled apoB-100 is present in milk 8 h after tail vein injection of $^{125}$I-TC-LDL. Shown is the PhosphorImage of SDS-PAGE separated injectate, serum, and whey.

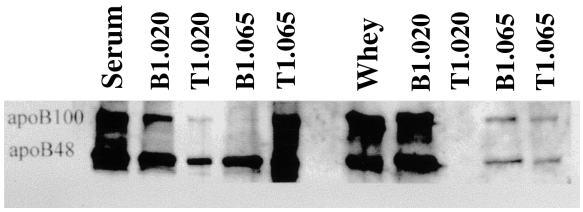


**Fig. 6.** Sequential density gradient centrifugation of lactating mouse serum and whey to isolate LDL. Shown are the top (T) and bottom (B) fractions of serum and whey centrifuged at a density of 1.020 g/ml, followed by recentrifugation at a density of 1.065 g/ml, analyzed for endogenous apoB by immunoblotting.

contained 6% of the total counts in whole milk, probably representing contamination with residual whey.

To determine whether the labeled protein had been degraded to smaller peptide fragments, three lactating mice were injected on day 10 with $^{125}$I-TC-LDL. After 8 h, blood and milk were collected, and serum and whey were prepared. Initial substrate, serum, and whey were separated by sodium dodecyl sulfate polyacrylamide gel electrophoresis (SDS-PAGE), as described in Materials and Methods. The gel was dried and imaged on the PhosphorImager (**Fig. 5**). The radioactivity was present in a protein band with the same mobility as the $^{125}$I-TC-LDL that had been injected into the animal. Smaller, labeled fragments were not observed. This finding indicates that the apoB component of the labeled LDL passed from the plasma into the milk with no perceptible degradation.

### Characterization of the apoB-containing particle in milk

Next we examined mouse milk for the presence of endogenous apoB. Whey was prepared, as described in Materials and Methods, from milk collected from normal CD-1 mice and subjected to sequential density ultracentrifugation. **Figure 6** shows that anti-rat LDL immunoreacts with two bands, corresponding to endogenous apoB-48 and apoB-100, in both serum and whey. Two bands were detected in the infranatant (B) but not the supernatant (T) of whey centrifuged at a density of 1.020 g/ml. However, both bands were detected in both the supernatant and infranatant of whey ultracentrifuged at 1.065 g/ml. This finding suggested that apoB-containing particles of a density falling in the LDL range are present in mouse milk. We named this particle the milk lipoprotein particle (MLP) and present further characterization of its properties below.

Different results were achieved with the serum separation. In this fed state, most of the particles that floated at 1.020 g/ml and most of the particles that sank at 1.065 g/ml contained only apoB-48, consistent with the presence of chylomicrons and chylomicron remnants, respectively.

The whey-to-serum ratio of endogenous apoB, quantitated by densitometry of Western blots of dilutions of whey and serum from two mice, was 0.34. This ratio is only slightly larger than the whey-to-serum ratio of labeled LDL of 0.21 ± 0.05 obtained from the uptake experiments, giving us confidence that the results obtained with human $^{125}$I-TC-LDL under non-steady-state conditions are reasonably representative of the fate of endogenous mouse LDL.

### Analysis of lipoproteins in mouse serum and whey

To analyze the size of the MLP, we separated lipoproteins from serum and whey by liquid chromatography. The serum from lactating mice had levels of all lipoprotein subspecies similar to those from serum from nonpregnant, nonlactating (NPNL) mice (**Fig. 7A**). In the elution range characterized by two IDL/LDL peaks in the serum, there was only a single, broad peak in the whey profile eluting slightly ahead of the major LDL peak in the plasma (peaks 2 and 3). The peak fraction of each of these populations was analyzed by SDS-PAGE, followed by immunoblotting. ApoB-48 and apoB-100 were present in the peaks corresponding to LDL-sized particles in whey as well as in serum from both lactating and NPNL mice (Fig. 7B).

In addition to analyzing the peaks for apoB, we carried out cholesterol and triglyceride analyses on fractions collected from the FPLC separation (Fig. 7C). As expected, the triglyceride in the serum of NPNL and lactating mice was associated with the VLDL/chylomicron peak (peak 1 in Fig. 7A). The cholesterol was associated with small, HDL-sized particles in the serum of NPNL mice (peak 4), but with a broad range of LDL- and HDL-sized particles in the serum of lactating mice (peaks 3 and 4). In the whey, however, significant amounts of triglyceride and cholesterol were associated only with peak 1. These large particles are likely to be a subpopulation of secreted milk fat globules (27), small enough to partition in the whey during high-speed centrifugation but large enough to be cleared in the void volume of the FPLC. This conclusion is supported by the finding that the milk fat globule proteins, xanthine oxidase and adipophilin, were associated with this peak (data not shown).

To further characterize the density of the MLP, density-gradient ultracentrifugation of pooled serum and whey from lactating CD1 mice was carried out as described in Materials and Methods, and the resulting gradient fractions were immunoblotted for endogenous mouse apoB. The results again showed that both apoB-48- and apoB-

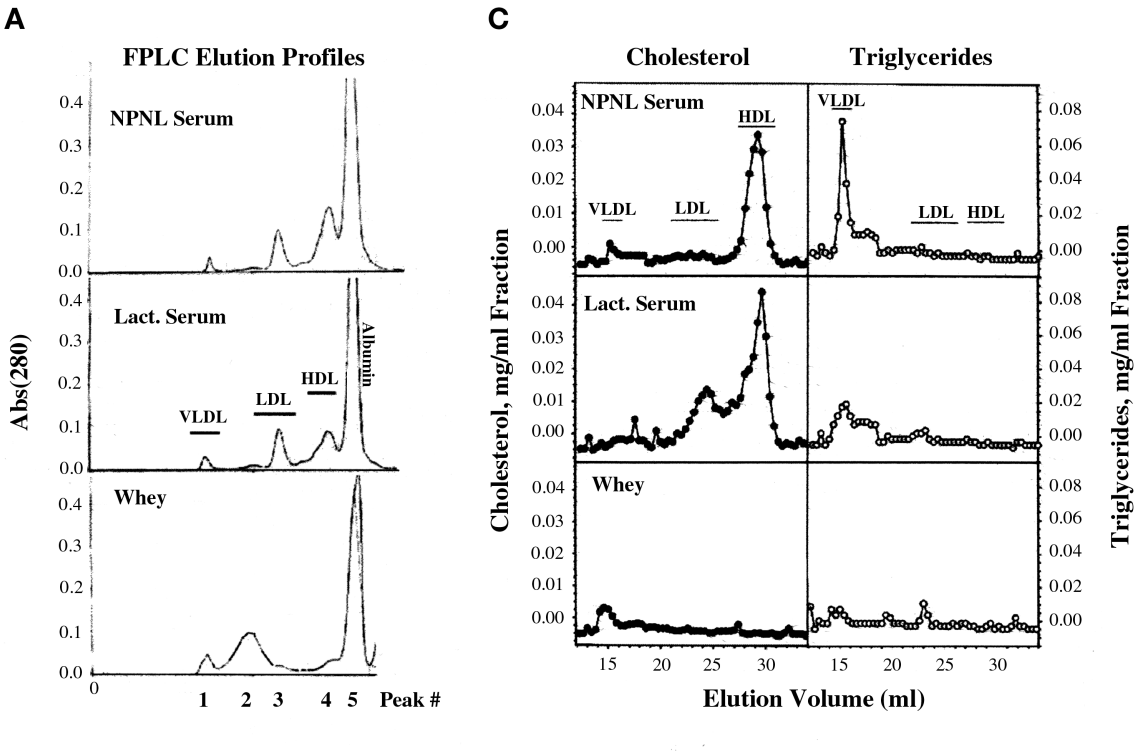


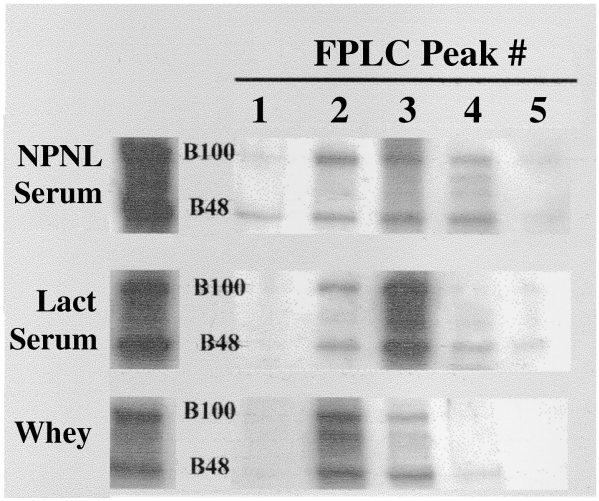


**Fig. 7.** Fast protein liquid chromatography (FPLC) separation of lipoproteins from whey and serum of NPNL, and lactating mice. A: Separation of serum and whey by FPLC as in Materials and Methods. Shown is the absorbance at 280 nm of eluting fractions. Peaks corresponding to VLDL (1), IDL/LDL (2 and 3), HDL (4), and albumin (5) are labeled. B: Western blot analysis of FPLC peak fractions from A showing the presence of endogenous apoB-100 and apoB48. C: Quantitation of total cholesterol and triglyceride in FPLC fractions.

100-containing particles are present in the whey but that these particles have a density >1.040 g/ml (**Fig. 8A**). Particles that span the LDL-density range are present in the serum of these mice. These density-gradient fractions of the whey were further analyzed for the presence of phospholipids (Fig. 8B). The apoB-containing fractions do contain phospholipids that are possibly responsible for the floatation of the MLP in the absence of associated cholesterol or triglyceride.

Density-gradient fractions from the NPNL serum, lactating mouse serum, or whey separations were separated by SDS-PAGE, and the proteins were stained with colloidal Coomassie blue (Fig. 8C). The banding pattern of the lightest serum LDL is simple, with only the apoB-48 staining, although Western blotting shows apoB-100 to be present as well (Fig. 8A). However, the lightest MLP shows many associated protein bands in addition to the apoB-48 band. Some of these could be major milk proteins that did not "wash" off of the MLP; albumin is particularly apparent. However, the more dense LDL from mouse serum also have more associated proteins (or these fractions are contaminated with other lipoproteins), many of which are also present on the MLP. This result suggests that these dense serum LDL particles may be transported preferentially across the mammary epithelium and deposited into the milk.

### Visualization of LDL interaction with the lactating mammary epithelium

Density-gradient centrifugation verifies that the MLP in the whey have an average density greater than 1.040 g/ml

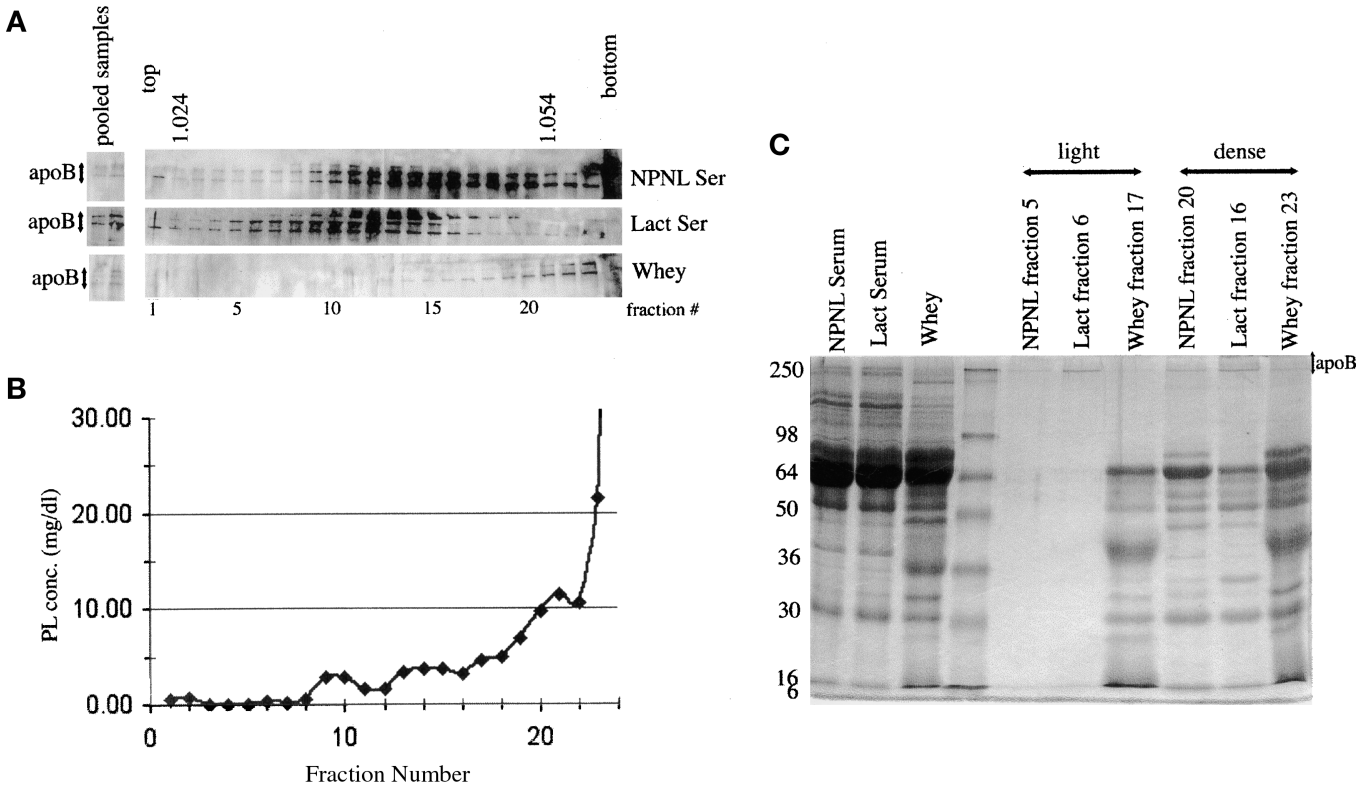


**Fig. 8.** Density-gradient centrifugation of mouse serum and whey. A: Western blot analysis for apoB in the density gradient fractions across the LDL density range. Densities in g/ml are shown at the top. B: Phospholipid analysis of the gradient fractions from the whey separation. C: Coomassie stain of density gradient fractions containing apoB. The original pooled NPNL serum and Lact serum and whey are compared with light and dense LDL/MLP from the density gradient fractions as shown in the figure. Molecular weight standards are shown in the unlabeled lane.

(Fig. 8A), and analysis of FPLC fractions shows that little cholesterol or triglyceride is associated with the MLP (Fig. 7). These findings suggest that the lactating mammary epithelium either takes up and transcytoses remnant LDL particles or generates these remnants by scavenging cholesterol from them in the process of transporting the LDL to the milk. To visualize the sorting of the cholesterol from the apoB, we utilized human LDL particles labeled with both DiI, noncovalently incorporated into the lipid phase, and FITC, covalently bound to the apoB protein moiety. The basal surface of the mammary epithelial cell from CD1 and LDLR-null mice was exposed in situ to this probe, as described in Materials and Methods, and processed for fluorescence microscopy to visualize the interaction of the probe with the lactating mammary gland. Frozen sections of mammary gland from both CD-1 and LDLR-null mice are shown in **Fig. 9A**. Fluorescence from the FITC and DiI channels is shown separately, in black and white as generated in the original image acquisition and overlaid, in pseudocolor, counterstained with DAPI to visualize nuclei. FITC staining of the basal surface of the cell suggests binding of the FITC-apoB to the membrane. Within the mammary epithelial cell, some endocytosis of whole particle can be detected by the presence of doubly stained vesicles (shown in yellow). However, a large amount of DiI (arrowheads) is localized independently from the apoB. DiI was also visualized in secreted milk fat globules (asterisks), suggesting intracellular trafficking of the lipid to the globules or globule membranes. DiI-depleted lipoproteins are evident as small green vesicles (small arrows). Quantitative analysis shows that the ratio of FITC to DiI fluorescence in the probe, as well as on the membrane of both strains of mice, is about 2:1 (probe, 1.96 ± 0.36; CD-1 membrane, 1.96 ± 0.08; LDLR-null membrane, 1.75 ± 0.69). However, intracellular staining is enriched for DiI in both strains (FITC/DiI ratios: CD-1 intracellular, 0.82 ± 0.06; LDLR-null intracellular, 0.65 ± 0.21). These data support the hypothesis that DiI is separated from the FITC-apoB protein moiety at or near the basal membrane of the mammary epithelial cell and that the LDLR is not involved in the process.

## DISCUSSION

We have shown that $^{125}$I-TC-labeled human LDL is taken up by the mouse mammary gland in increasing amounts over the course of reproductive development of the gland. A portion of this labeled apoB is deposited into the milk, as is endogenous LDL. Utilizing serum apoB levels given in the literature for NPNL FVB mice (28) and the estimated steady state ratio of apoB of about 0.34, we estimate that the mouse mammary gland transcytoses about 50 μg of apoB into milk per day, a substantial rate of transcytosis.

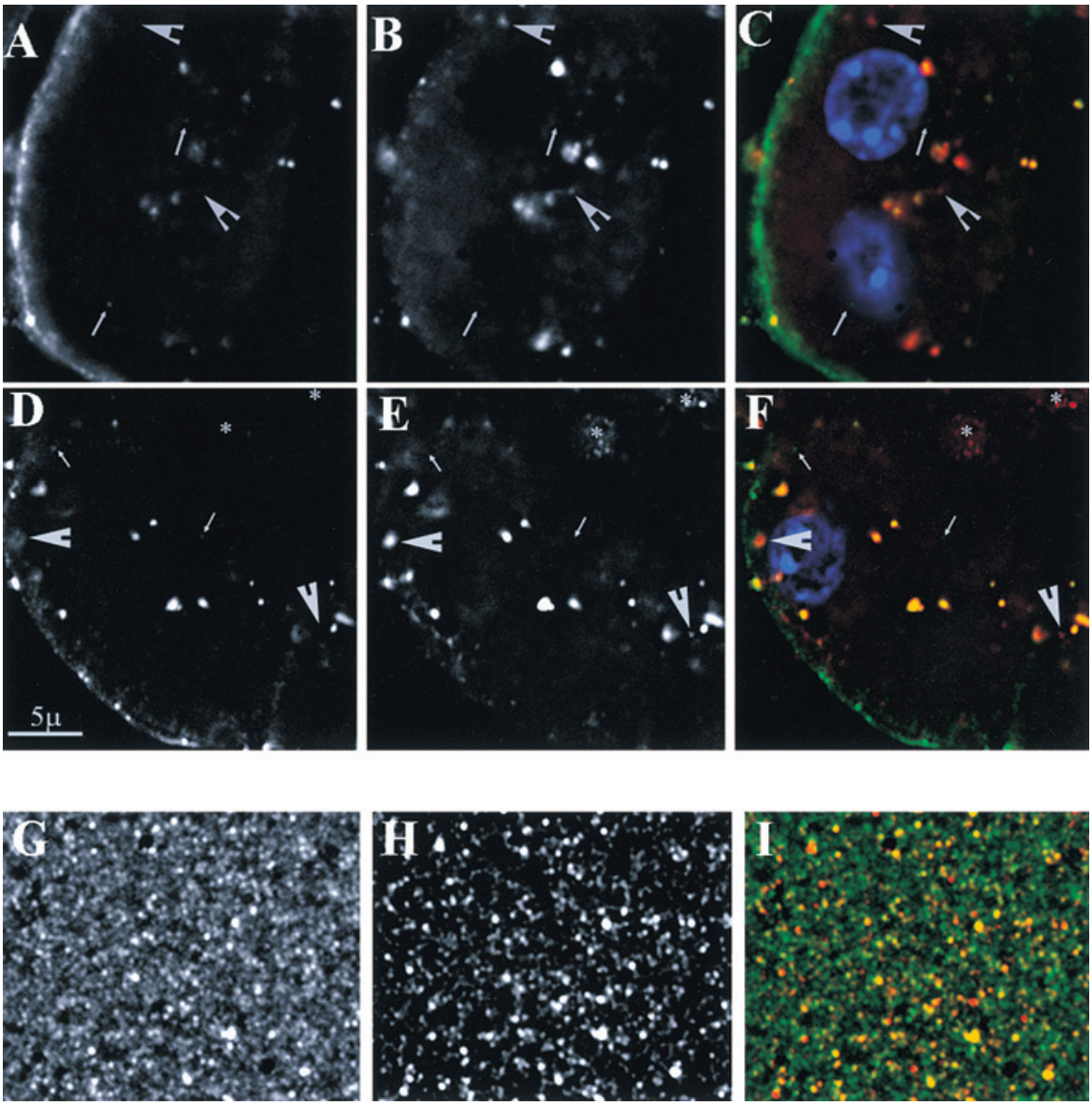


**Fig. 9.** Interaction of fluoresceinated (FITC) and DiI labeled LDL with mammary epithelial cells. A–C: CD-1 mouse; D–F:, LDLR-null mouse; G–I: labeled LDL probe. To show the primary image data, FITC-apoB is shown in black and white (A, D, and G) and in green in the overlays (C, F, and I). DiI is shown in black and white (B, E, and H) and in red on the overlay. Co-localization of the two probes appears yellow in the overlay where nuclei stained with DAPI are shown in blue. The basal surface of the mammary epithelial cell is on the bottom left of frames A–F. The apical membrane and milk space are on the top right side of these frames. Small arrows indicate vesicles containing apoB only, and large arrowheads denote organelles containing DiI only. Asterisks indicate labeled milk fat globules in the lumen. G–I: Visualization of the initial probe suspended in mounting medium. All images were captured, deconvolved, and scaled similarly as described in Materials and Methods.

The MLP appear to have little associated triglyceride or cholesterol, but they do contain residual phospholipids. The presumed sorting of the protein moiety from the lipid phase by the mammary epithelial cell was mimicked by the separation of the FITC from the DiI in doubly labeled human LDL. Our data show that this process also occurs in the LDLR-null mouse, indicating that it is not dependent on the presence of the LDLR.

It is not surprising that the mammary gland increases its uptake of cholesterol and triglycerides during pregnancy and lactation. During the reproductive cycle, the mammary gland goes from a largely quiescent tissue comprised predominantly of lipid-filled adipocytes (virgin state) to one comprised largely of mammary epithelial cells within a fat pad (late pregnant). After parturition, it becomes an actively secreting gland composed primarily of epithelial cells within a fat-depleted adipocyte stroma (lactating). Thus, pregnancy is accompanied by extensive epithelial cell proliferation and growth of the gland requiring new membrane synthesis. Lactation is accompanied by secretion of an enormous amount of lipid into the milk. Over the course of a 21-day lactation, a female mouse nursing a large litter will produce about 20 g of milk fat, containing about 100 mg of cholesterol. Smith et al. (29) studied the effect of lactation on plasma lipoproteins in rats. Whereas the LDL content of plasma was increased in lactation, very

low density lipoprotein (VLDL)-sized particles were not apparent. Correspondingly, the rats were hypercholesterolemic, with very low levels of circulating triglycerides. Twenty-four hours after weaning the rat pups, the profile was reversed, with many very large VLDL-sized particles in the circulation and no detectable LDL. This rapid change demonstrates the requirement of the lactating mammary gland for large amounts of triglyceride but does not address the clearance of LDL particles from the circulation. Smith et al. saw a 1.5-fold increase in LDLR expression in the livers of lactating rats, but hepatic concentrations of triglycerides and free and esterified cholesterol were unchanged. Their conclusion was that decreased amounts of plasma lipoproteins were being cycled back to the liver during lactation. Our data (Fig. 3B) are consistent with this conclusion.

Although data on expression of any members of the LDLR family in mammary epithelial cells are not available, we expected LDL uptake to involve the classic LDLR endocytic pathway with targeting to the lysosome, processing of the lipid by lysosomal acid lipase, and degradation of the apoB by proteases (8). Instead, at least part of the labeled apoB appears intact in the milk associated with a particle, the MLP, that was denser and larger than most serum LDL but contained little triglyceride or cholesterol. Further, apoB uptake and secretion were not different in the LDLR-null mouse.

To visualize the interaction of LDL with the mammary epithelial cell, we incubated doubly labeled LDL, with both the protein and lipid moieties fluorescently tagged, with the in situ, lactating mammary gland. We found that both protein and lipid were present at the basal membrane, but most of the lipid appeared to be internalized separately, suggesting that the mammary epithelium scavenges lipid from LDL via a selective uptake pathway. Selective lipid uptake has been described in other cell types, primarily utilizing the scavenger receptors (9, 11–13, 28, 30–32). It is not known whether mammary epithelial cells express the members of the class B scavenger receptor family, SR-BI and SR-BII, but SR-BI mRNA and protein have been shown to be increased in the whole mammary gland of the pregnant rat (10). In addition, another member of this family, CD36, is expressed on mammary epithelial cells and is present on milk fat globule membranes (33–35). CD36 can bind many protein and lipid ligands (36–40), and a role in long-chain fatty acid uptake has been demonstrated (41, 42). Other potential mediators of binding, processing, or uptake of LDL include cholesterol ester transfer protein (43) and apoE (44), lipoprotein lipase (45), and the syndecan family of heparan sulfate proteoglycans (46, 47), all of which have been implicated in lipoprotein clearance in other tissues.

Obviously there is much work to be done to determine the mechanisms by which LDL is processed by the mammary gland and apoB deposited in the milk and to what extent LDL does deliver the cholesterol to the mammary gland. The milk-to-serum ratio of apoB is only about 0.34, whereas the milk-to-serum cholesterol ratio is about 2.4, implying that less than 15% of the cholesterol in milk is derived from the MLP. Whereas there is evidence for de novo cholesterol synthesis in the mammary gland (6), no quantitative data as to the extent of this process are available for the mouse.

Our experiments show that the lactating mammary epithelial cell may have unique mechanisms of processing plasma lipoproteins. It appears both to take up lipids from LDL at the plasma membrane and to internalize the lipoprotein particle. Internalization is not, however, accompanied by degradation of the protein moiety; instead, the endocytosed particle is targeted for transcytosis and deposited in the milk. It is not known whether ingestion of the MLP is beneficial to the neonate or whether the process is an efficient way to clear the particles from the circulation. Further experiments are necessary to complete our understanding of both mammary uptake mechanisms and of maternal adaptation to this special metabolic state.

We thank Dr. D. Ambrusco and T. Paine for collecting serum from patients with familial hypercholesterolemia and the Metabolic Core Laboratory of the Colorado Clinical Nutrition Research Unit (NIH DK 48520) for performing lipid assays on the fractionated lipoproteins. This work was supported by USDA Grant 9303441 and NIH Grant R37 HD 15437.

*Manuscript received 23 July 1999, in revised form 5 June 2000, and in re-revised form 11 December 2000.*

## REFERENCES

1. Hamosh, M. 1995. Enzymes in human milk. In: Handbook of Milk Composition. R. G. Jensen, editor. Academic Press, San Diego. 388–427.
2. Dils, R. R. 1983. Milk fat synthesis. In: Biochemistry of Lactation. T. B. Mepham, editor. Elsevier Science Publishers B.V., Amsterdam. 142–157.
3. Jensen, D. R., S. Gavigan, V. Sawicki, D. L. Witsell, R. H. Eckel, and M. C. Neville. 1994. Regulation of lipoprotein lipase activity and mRNA in the mammary gland of the lactating mouse. *Biochem. J.* **298:** 321–327.
4. Popjak, G., T. H. French, and S. J. Folley. 1951. Utilization of acetate for milk-fat synthesis in the lactating goat. *Biochem. J.* **48:** 411–416.
5. Raphael, B. C., S. Patton, and R. D. McCarthy. 1975. The serum lipoproteins as a source of milk cholesterol. *FEBS Lett.* **58:** 42–49.
6. Long, C. A., S. Patton, and R. D. McCarthy. 1980. Origins of the cholesterol in milk. *Lipids.* **15:** 853–857.
7. Goldstein, J. L., M. S. Brown, R. G. Anderson, D. W. Russell, and W. J. Schneider. 1985. Receptor-mediated endocytosis: Concepts emerging from the LDL receptor system. *Ann. Rev. Cell. Biol.* **1:** 1–39.
8. Acton, S., A. Rigotti, K. T. Landschulz, S. Xu, H. H. Hobbs, and M. Krieger. 1996. Identification of scavenger receptor SR-BI as a high density lipoprotein receptor. *Science.* **271:** 518–520.
9. Azhar, S., A. Nomoto, S. Leers-Sucheta, and E. Reaven. 1998. Simultaneous induction of an HDL receptor protein (SR-BI) and the selective uptake of HDL-cholesteryl esters in a physiologically relevant steroidogenic cell model. *J. Lipid Res.* **39:** 1616–1628.
10. Landschulz, K. T., R. K. Pathak, A. Rigotti, M. Krieger, and H. H. Hobbs. 1996. Regulation of scavenger receptor, class B, type I, a high density lipoprotein receptor, in liver and steroidogenic tissues of the rat. *J.Clin. Invest.* **98:** 984–995.
11. Stangl, H., G. Cao, K. L. Wyne, and H. H. Hobbs. 1998. Scavenger Receptor, Class B, Type I-dependent stimulation of cholesterol esterification by high density lipoproteins, low density lipoproteins, and nonlipoprotein cholesterol. *J. Biol. Chem.* **273:** 31002–31008.
12. Swarnaker, S., R. E. Temel, M. A. Connelly, S. Azhar, and D. L. Williams. 1999. Scavenger receptor class B, type I, mediates selective uptake of low density lipoprotein cholesteryl ester. *J. Biol. Chem.* **274:** 29733–29739.
13. Fidge, N. H. 1999. High density lipoprotein receptors, binding proteins, and ligands. *J. Lipid Res.* **40:** 187–201.
14. Pittman, R. C., T. E. Carew, C. K. Glass, S. R. Green, C. A. Taylor, and A. D. Attie. 1983. A radioiodinated, intracellularly trapped ligand for determining the sites of plasma protein degradation in vivo. *Biochem. J.* **212:** 791–800.

15. Carew, T. E., R. C. Pittman, E. R. Marchand, and D. Steinberg. 1984. Measurement in vivo of irreversible degradation of low density lipoprotein in the rabbit aorta. *Arterioscler.* **4:** 214–224.
16. Ishibashi, S., M. S. Brown, J. L. Goldstein, R. D. Gerard, R. E. Hammer, and J. Herz. 1993. Hypercholesterolemia in low density lipoprotein receptor knockout mice and its reversal by adenovirus-mediated gene delivery. *J. Clin. Invest.* **92:** 883–893.
17. Ishibashi, S., J. L. Goldstein, M. S. Brown, J. Herz, and D. K. Burns. 1994. Massive xanthomatosis and atherosclerosis in cholesterol-fed low density lipoprotein receptor-negative mice. *J. Clin. Invest.* **93:** 1885–1893.
18. Redgrave, T. G., C. K. Roberts, and C. E. West. 1975. Separation of plasma lipoproteins by density gradient ultracentrifugation. *Anal. Biochem.* **65:** 42–49.
19. Berga, S. E., and M. C. Neville. 1985. Sodium and potassium distribution in the lactating mouse mammary gland *in vivo*. *J. Physiol.* **361:** 219–230.
20. Neville, M. C., and R. T. Mathias. 1979. The extracellular compartment of frog skeletal muscle. *J. Physiol.* **288:** 71–83.
21. Jiao, S., T. G. Cole, R. T. Kitchens, B. Pfleger, and G. Schonfeld. 1990. Genetic heterogeneity of lipoproteins in inbred strains of mice: analysis by gel-permeation chromatography. *Metabolism.* **39:** 155–160.
22. Ghosh, R. N., D. L. Gelman, and F. R. Maxfield. 1994. Quantification of low density lipoprotein and transferrin endocytic sorting in HEp2 cells using confocal microscopy. *J. Cell Science.* **107:** 2177–2189.
23. Ghosh, R. N., W. G. Mallet, T. T. Soe, T. E. McGraw, and F. R. Maxfield. 1998. An endocytosed TGN38 chimeric protein is delivered to the TGN after trafficking through the endocytic recycling compartment in CHO cells. *J. Cell Biol.* **142:** 923–936.
24. Jack, L. J., S. Kahl, D. L. St Germain, and A. V. Capuco. 1994. Tissue distribution and regulation of 5'-deiodinase processes in lactating rats. *J. Endocrinol.* **142:** 205–215.
25. Peaker, M. 1977. The aqueous phase of milk: ion and water transport. *Symp. Zool. Soc. London.* **41:** 113–134.
26. Huston, G. E., and S. Patton. 1986. Membrane distribution in human milks throughout lactation as revealed by phospholipid and cholesterol analyses. *J. Pediatr. Gastroenterol. Nutr.* **5:** 602–607.
27. Mather, I. H., and T. W. Keenan. 1998. Origin and secretion of milk lipids. *J. Mamm. Gland Biol. Neoplasia.* **3:** 259–273.
28. Ueda, Y., L. Royer, E. Gong, J. Zhang, P. N. Cooper, O. Francone, and E. M. Rubin. 1999. Lower plasma levels and accelerated clearance of high density lipoprotein (HDL) and Non-HDL cholesterol in scavenger receptor class B type I transgenic mice. *J. Biol. Chem.* **274:** 7165–7171.
29. Smith, J. L., S. R. Lear, T. M. Forte, W. Ko, M. Massimi, and S. K. Erickson. 1998. Effect of pregnancy and lactation on lipoprotein and cholesterol metabolism in the rat. *J. Lipid Res.* **39:** 2237–2249.
30. Plump, A. S., S. K. Erickson, W. Weng, J. S. Partin, J. L. Breslow, and D. L. Williams. 1996. Apolipoprotein A-I is required for cholesterol ester accumulation in steroidogenic cells and for normal adrenal steroid production. *J. Clin. Invest.* **97:** 2660–2671.
31. Sparrow, C. P., and R. C. Pittman. 1990. Cholesterol esters selectively taken up from high-density lipoproteins are hydrolyzed extralysosomally. *Biochim. Biophys. Acta.* **1043:** 203–210.
32. Webb, N. R., P. M. Connell, G. A. Graf, E. J. Smart, W. J. S. de Villiers, F. C. de Beer, and D. R. van der Westhuyzen. 1998. SR-BII, an isoform of the scavenger receptor BI containing an alternate cytoplasmic tail, mediates lipid transfer between high density lipoprotein and cells. *J. Biol. Chem.* **273:** 15241–15248.
33. Aoki, N., T. Ishii, S. Ohira, Y. Yamaguchi, M. Negi, T. Adachi, R. Nakamura, and T. Matsuda. 1997. Stage specific expression of milk fat globule membrane glycoproteins in mouse mammary gland: Comparison of MFG-8, butyrophilin, and CD36 with a major milk protein, beta-casein. *Biochim. Biophys. Acta.* **1334:** 182–190.
34. Berglund, L., T. E. Petersen, and J. T. Rasmussen. 1996. Structural characterization of bovine CD36 from the milk fat globule membrane. *Biochim. Biophys. Acta.* **1309:** 63–68.
35. Greenwalt, D. E., K. W. K. Watt, O. Y. So, and N. Jiwani. 1990. PAS IV, an integral membrane protein of mammary epithelial cells, is related to platelet and endothelial cell CD36 (GP IV). *Biochemistry.* **29:** 7054–7059.
36. Han, J., D. P. Hajjar, M. Febbraio, and A. C. Nicholson. 1997. Native and modified low density lipoproteins increase the functional expression of the macrophage class B scavenger receptor, CD36. *J. Biol. Chem.* **272:** 21654–21659.
37. Baillie, A. G. S., C. T. Coburn, and N. A. Abumrad. 1996. Reversible binding of long-chain fatty acids to purified FAT, the adipose CD36 homolog. *J. Membr. Biol.* **153:** 75–81.
38. Ryeom, S. W., R. L. Silverstein, A. Scotto, and J. R. Sparrow. 1996. Binding of anionic phospholipids to retinal pigment epithelium may be mediated by the scavenger receptor CD36. *J. Biol. Chem.* **271:** 20536–20539.
39. Rigotti, A., S. L. Acton, and M. Krieger. 1995. The Class B scavenger receptors SR-BI and CD36 are receptors for anionic phospholipids. *J. Biol. Chem.* **270:** 16221–16224.
40. Daviet, L., and J. L. McGregor. 1997. Vascular biology of CD36: Roles of this new adhesion molecule family in different disease states. *Thromb. Haemost.* **78:** 65–69.
41. Febbraio, M., N. A. Abumrad, D. P. Hajjar, K. Sharma, W. Cheng, S. F. A. Pearce, and R. L. Silverstein. 1999. A null mutation in murine CD36 reveals an important role in fatty acid and lipoprotein metabolism. *J. Biol. Chem.* **274:** 19055–19062.
42. Abumrad, N. A., M. R. El-Maghrabi, E. Z. Amri, E. Lopez, and P. A. Grimaldi. 1993. Cloning of a rat adipocyte membrane protein implicated in binding or transport of long-chain fatty acids that is induced during preadipocyte differentiation: Homology with human CD36. *J. Biol. Chem.* **268:** 17665–17668.
43. Benoist, F., P. Lau, M. McDonnell, H. Doelle, R. Milne, and R. McPherson. 1997. Cholesterol ester transfer protein mediates selective uptake of high density lipoprotein cholesterol esters by human adipose tissue. *J. Biol. Chem.* **272:** 23572–23577.
44. Swarnakar, S., M. E. Reyland, J. Deng, S. Azhar, and D. L. Williams. 1998. Selective uptake of low density lipoprotein-cholesterol ester is enhanced by inducible Apolipoprotein E expression in cultured mouse adrenocortical cells. *J. Biol. Chem.* **273:** 12140–12147.
45. Olivecrona, T., and G. Bengtsson-Olivecrona. 1993. Lipoprotein lipase and hepatic lipase. *Curr. Opin. Lipidol.* **4:** 187–196.
46. Jalkanen, M., A. Rapraeger, S. Saunders, and M. Bernfield. 1987. Cell Surface Proteoglycan of mouse mammary epithelial cells is shed by cleavage of its matrix-binding ectodomain from its membrane-associated domain. *J. Cell Biol.* **105:** 3087–3096.
47. Saunders, S., M. Jalkanen, S. O'Farrell, and M. Bernfield. 1989. Molecular cloning of syndecan, an integral membrane proteoglycan. *J. Cell Biol.* **108:** 1547–1556.